Deep adversarial attack on target detection systems

Uche M. Osahor and Nasser M. Nasrabadi

Lane Department of Computer Science and Electrical Engineering, West Virginia University, Morgantown, USA

1. ABSTRACT

Target detection systems identify targets by localizing their coordinates on the input image of interest. This is ideally achieved by labeling each pixel in an image as a background or a potential target pixel. Deep Convolutional Neural Network (DCNN) classifiers have proven to be successful tools for computer vision applications. However, prior research confirms that even state of the art classifier models are susceptible to adversarial attacks. In this paper, we show how to generate adversarial infrared images by adding small perturbations to the targets region to deceive a DCNN-based target detector at remarkable levels. We demonstrate significant progress in developing visually imperceptible adversarial infrared images where the targets are visually recognizable by an expert but a DCNN-based target detector cannot detect the targets in the image.

2. INTRODUCTION

Deep learning remains one of the greatest achievements and still makes significant progress in artificial intelligence.[?,?,?] It has found value in a wide domain of machine learning applications, ranging from image classification, object detection, speech recognition, voice synthesis, biometric recognition and security, etc.[?,?,?] With the plethora of data flying about, deep learning remains the best choice for such computational demands. The complexity of managing data as well as the need for hardware acceleration will make the aforementioned fields an obvious area of interest with unending innovative ways to solve challenges as they arise.

Object detection is a technology that deals with detecting of objects from images. It has been widely applied in many fields including object tracking, autonomous driving and intelligent video surveillance. The technique of deep neural networks (DCNNs) has aided the development of object detection. However, DCNNs are known to be vulnerable to adversarial examples.

Object detection represents key components of many vision-based applications, from surveillance to vehicle navigation, autonomous vehicle navigation, etc. Hence, a number of algorithms have been proposed to cope with issues related to variations in objects' appearance, occlusion conditions, sensor and so on.[?] Most research works have focused on the visible light spectrum, by developing effective solutions tailored to both single and multiple monocular or stereo cameras. Unfortunately, these approaches are based solely on visible scenes. Recently, technological advancements have led to an important reduction in the production costs of infrared (IR) light sensors. Hence, infrared cameras, have found more prominence in target detection and recognition systems. Attention has been drawn to long-wave infrared (LWIR) light in the range 8–12 nm and to forward looking infrared (FLIR) sensors, because of their ability to clearly represent heat sources at night or through smoke, fog, haze, etc.[?]

In FLIR images, the intensity of an object depends on its temperature and radiated heat and it is not influenced by light conditions and object surface features which are key to visible light sensors. An approach that is frequently pursued in target detection consists in fusing information coming from both visible and IR image sets. Thus, maximizing the positive benefits of their strong points while limiting at the same time the impact of their constraints. In practice, when detecting pedestrians in visible light imagery, clothes color may be used to resolve possible occlusions that may occur and at night, an IR sensor would help to deal with the lack of color information. Detection and tracking in FLIR images are complicated by other important factors. In fact, real-life images captured by surveillance cameras, Unmanned Aerial Vehicles (UAVs) and other stationary and non-stationary sensors are generally characterized by limited resolution, poor contrast and low signal-to-noise

email: nasser.nasrabadi@mail.wvu.edu,uo0002@mix.wvu.edu

ratio.[?,?] Nonetheless, important features could be observed as well. There exist challenges that are almost shared between the infrared and visible domain. For instance, in pedestrian detection and tracking, both the visible light and IR techniques have to cope with the difficulties associated with a signature that is continuously changing due to the non-rigid frame of the human body and whose trajectories are difficult to predict because of the intrinsic gait complexity of human walking motion and social behaviors.[?]

However, DCNN architectures have always been developed based on the task of interest, the content within the layers of a typical network defines the potential output from the entire network. For object detection tasks, the model architecture can be divided into two main categories: one-stage detectors and two-stage detectors. The one-stage detectors adapt a sliding window approach across the image and applies anchors(bounding boxes) at several locations of feature maps created by the network model.[?] A collection of feature maps are divided into different spatial locations and at each locale, anchors are assigned respectively. These anchors are boxes with fixed scales and ratios to capture objects of different shapes and sizes along the grid points of the target image. If four different scales and four ratios are being used, a total of 16 anchors are assigned to each specific location. The anchor scales and ratios are hyper-parameters, these anchors are then classified to produce predictions and the coordinates of the boxes are regressed.[?] The output from each fine tuned anchor box is a classification score and bounding box coordinate. To avoid detecting the same object multiple times, non-maximum suppression is employed, which groups overlapping detection of the same objects into one detection. The two-stage detector systems consists of two networks. One network, called region proposal network,extracts the interesting regions in the image where targets of interest are most likely to be found and then a second network to classify these regions into target or background. An example of two stage detectors is the deep target detector.[?] Most two-stage detectors usually show better performance than one-stage detectors[?] but have a higher computational time. Recent papers have been suggesting that the gap between one-stage and two-stage are shrinking when it comes to the trade-off between prediction time and computational complexity.

Fast R-CNN[?] is a Fast Region-based Convolutional Network method (Fast R-CNN) for object detection. In this algorithm, an input image and multiple regions of interest (ROIs) are fed into a convolutional neural network. Each ROI is pooled into a fixed-size feature map and then mapped to a feature vector by several fully connected layers (FCs). The network contains two output vectors per ROI: softmax probabilities and per-class bounding-box regression offsets.

Faster R-CNN[?] improved on the performance of Fast R-CNN by introducing a region proposal Network (RPN) that exploits the full-image convolutional features with the detection network, thus enabling nearly cost-free region proposals. An RPN is a network that simultaneously predicts object bounding boxes and scores at each position. RPNs are trained end-to-end to generate high quality region proposals. This network outpaces the fast R-CNN because the region proposal network are fused and could be trained end to end.

YoLo Detector (You only look once)[?] is a newer approach to do object detection. Previous work on object detection make classifiers detection. Instead, YoLo adapts object detection as a regression problem to spatially separated bounding boxes and associated class probabilities. A neural network predicts bounding boxes and class probabilities from full images in one evaluation shot. Since the whole detection pipeline is a single network, it can be optimized end-to-end directly on detection performance. The unified architecture is extremely fast but not as accurate as Faster R-CNN. However, Yolo is limited[?] because its predefined grid cells' aspect ratio is fixed. SSD (Single shot detector)[?] successfully fixed that by permitting more aspect ratios. Hence, SSD boxes can bound objects in a tighter, more accuracy fashion. Another improvement is that SSD adds more convolutional layers after VGG for detection instead of two fully connected layers like YOLO. Compared to other single stage methods, SSD has much better accuracy, even with a smaller input image size.

As deep neural networks have etched their path in numerous labs to real world applications, the security and integrity of such applications have proven to be a major problem.[?,?,?] Sadly, recent studies have clearly indicated that deep neural networks are also susceptible to attacks.[?] This vulnerability has posed a huge concern for the future of machine learning as a whole, this is because real time critical applications like self driving cars, unarmed aerial vehicles tracking, target recognition etc are pretty sensitive to errors, which could result to human casualty.

Szegedy et al.[?] first discovered this adversarial flaw in deep networks, they created small perturbations on the images for the image classification problem and successfully fooled state-of-the-art deep neural networks at

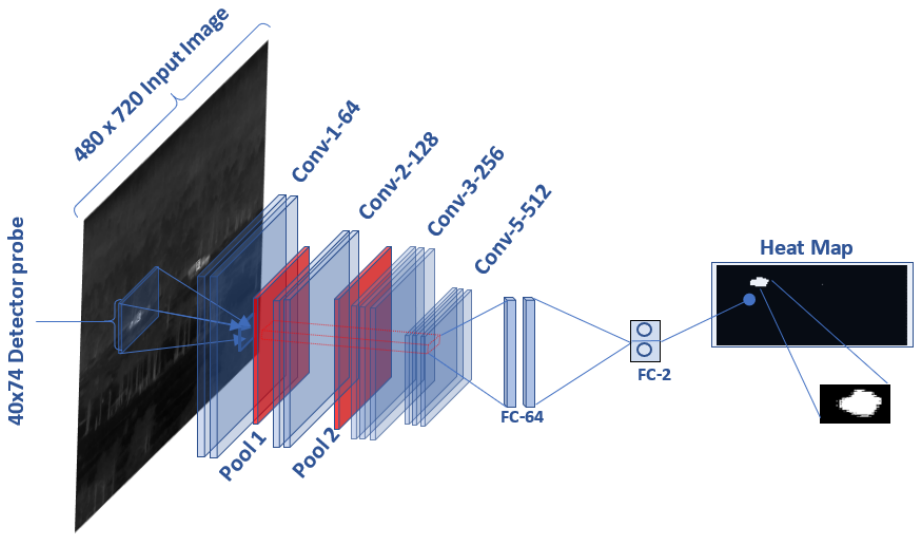

Figure 1: A DCNN-based target detector architecture. The network is trained to detect target chips (40x74) from clutter. At test phase, the detector probe strides across the 480x470 image to generate a heat map representing the output of the detector from an image containing adversarial target chips (target region with adversarial patch).

remarkable ratings. They based their rationale on the extreme nonlinearity of deep neural networks. However, Goodfellow et al.[?] provided detailed analysis with supportive experiments that suggest linearity is a better claim for the adversarial vulnerability of deep networks. Papernot et al.[?] addressed the aspect of generalization of adversarial examples while Hitaj et al.[?] exploited the nature of learning models to train adversarial networks. A Deep neural network remains somewhat of a black box of complexities that has led scientists and engineers on developing various techniques to peer into the endless depth of abstractions. Many papers have tried to interpret these networks with significant progress, from investigating such adversarial examples more knowledge could be developed to understand adversarial attacks even better.[?]

Kurakin et al.[?] demonstrated that when adversarial examples are printed out, an adversarially crafted image will continue to be adversarial to classifiers even under different lighting and orientations. Athalye et al.[?] demonstrated how adversarial objects can be 3D printed and misclassified by networks at different orientations and scales. Their adversarial examples were designed to be perturbations of a normal object (e.g. a turtle that has been adversarially perturbed to be classified as a rifle). Sharif et al.[?] also showed that one can fool facial recognition software by constructing adversarial glasses. These glasses were crafted to impersonate any person, but were custom made for the attacker's face. Recently, Evtimov et al.[?] demonstrated a couple of methods for constructing stop signs that are misclassified by DCNN models, either by printing out a large poster that looks like a stop sign, or by placing adversarial stickers on a stop sign. Most work focused on attacking and defending against either small or imperceptible changes to the input.

In this paper, we built a DCNN target detector using a VGG16 architecture[?] that performed at over 99% in accuracy, capable of distinguishing a target chip from background chip. We further crafted adversarial patches to attack our VGG-16 based detector network. These adversarial images were created by adding them as an adversarial patch to each target region in each test dataset. A sliding frame was built to stride across the full image from the test dataset containing the targets with adversarial patches, a resulting heat-map was produced as the output of the detection system (Figure 1), showing the a drop in detection performance due to the adversarial properties. Our experiments recorded promising results that highlight the dangers of adversarial attacks on detection systems.

3. CRAFTING ADVERSARIAL EXAMPLES

In this section, we identify some adversarial techniques and principles behind our adversarial attack. A myriad of concepts have being developed to attack deep neural networks. In most attack scenarios, the attacker wants to mis-classify the image of interest, without altering a human's ability to classify it.

Goodfellow et al.[?] proposed a new strategy named Fast Gradient Sign Method (FGSM) to craft adversarial examples. They implemented their algorithm against the famous GoogLeNet architecture.[?] The method took advantage of the linearity property of DCNNs and was capable of computing adversarial perturbations efficiently. The perturbation is expressed as:

$$\eta = \epsilon sign(\nabla_x J_\theta(x, l)), \tag{1}$$

where ϵ is the magnitude of the perturbation. The generated adversarial sample x_0 is calculated as: $x_0 = x + \eta$. The slight alterations to the original image is difficult to be spotted by a human eye. However, a large ϵ is likely to introduce noticeable perturbations but can get more adversarial samples especially when the original images are simple (MNIST Dataset).

Similar concepts of fast gradient sign method were implemented in similar manner. Yingpeng et al.[?] applied momentum to FGSM to generate examples more iteratively. The gradients were calculated by:

$$g_{t+1} = \mu g_t + \frac{\nabla_x J(x_t, l)}{\|\nabla_x J(x_t, l\|}. \tag{2}$$

They claimed that the introduction of momentum considerably improves the effectiveness of attack and transferability by applying the on-step attack and the ensembling method. Kurakin et al.[?]also introduced a method called One-step Target Class Method (OTCM), it showed decent improvements to the FGSM technique by increasing the probability of the target class:

$$x' = x - \epsilon sign(\nabla_x J(\theta, x, l)). \tag{3}$$

Moosavi-Dezfooli et al.[?] came up with the DeepFool algorithm to find small perturbations that are sufficient to change the classification result. The original image x_0 was manipulated iteratively. At each iteration of the algorithm, the perturbation for x_0 that reaches the decision boundary is computed and updated for corresponding epochs. DeepFool[?] is implemented as an optimization technique which can yield a good approximation of the minimal perturbation. They performed some attack experiments against several DCNN image classifiers, such as GoogLeNet, ResNet, AlexNet etc. Their work demonstrated that DeepFool could craft a smaller perturbation than FGSM, which however is still effective to trick the target models.

Carlini and Wagner[?] also employed an optimization algorithm to seek possible imperceptible perturbations. They came up with three powerful attacks for the L_0, L_2, and L_∞ distance metrics. Using popular datasets, such as MNIST and ImageNet, they trained deep network models to evaluate their attack strategy. As demonstrated in[?] CW attacks can find closer adversarial examples than the other attack techniques and never fail to find an adversarial example.

4. EVALUATION

4.1 Dataset

In this paper, the dataset of choice is the Comanche FLIR dataset. Its a collection of multiple targets captured at different angular orientation and range. The dataset is divided into SIG and ROI. The dataset comprises of 10 different targets denoted as tg1 to tg10. Each target is subdivided into 72 orientations, corresponding to angles of 0° to 355°in azimuth orientation. The SIG dataset were acquired over favorable conditions and has over 13,800 target images at 10-bit gray-scale. The images are 480x720 and target images (chips) cropped at

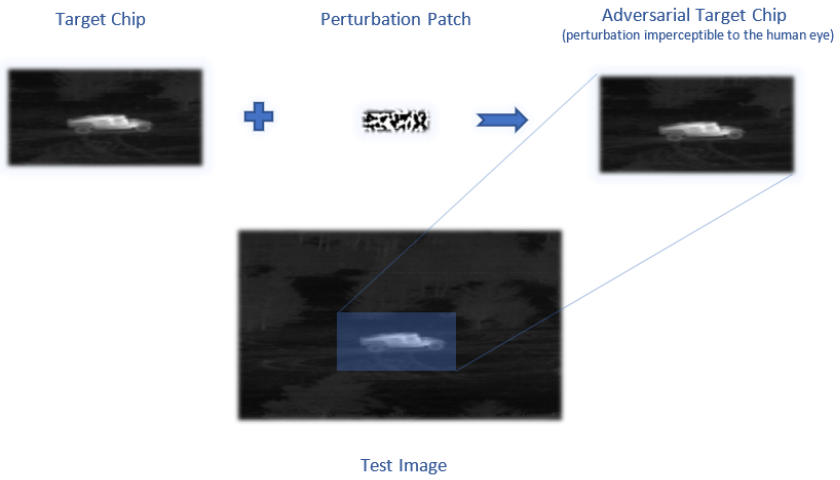

Figure 2: Crafting a test image with an adversarial patch. A target chip of size 40x74 (top left) is used as the input template for adversarial crafting. The adversarial perturbation (middle) is crafted from the target chip region of interest for the side, frontal and back view respectively. The result is a perturbation patch(imperceptible to the human eye) that is attached as a patch to the 480x720 image region of interest, thereby resulting is an image consisting of an adversarial patch(right). A complete 480x720 image with adversarial perturbation is shown in the bottom image.

40x74. Over 5000 clutter chips were also created to improve the training performance. Due to the nature of the DCNN architecture, the 40x75 target chips were resized to 40x74 due to the two max pooling layers and striding.[?] The chips were randomly partitioned with 75% set for training and 25% for testing. We implemented data augmentation techniques to double the dataset in order to maximize detection performance. The ROI consists of data obtained at less favorable conditions such as varying weather conditions, different backgrounds, within and around clutter. The images were captured at cold and hot scenes and at different distances (ranging from 688 to 3403 meters) to add some diversity to the database.[?]

4.2 Attack Approach

In this paper, we apply the FGSM strategy[?] by finding a targeted adversarial example. Using our DCNN detector $P[y|x]$, with input $x \epsilon R^N$, arbitrary target class y_b and a maximum perturbation ϵ, we seek to find an input x_b that maximizes the log $(P[y_b|x_b])$, subject to the constraint that $\|x - x_b\|_\infty \leq \epsilon$. We parameterize $P[y|x]$ by our DCNN to perform gradient descent on x in order to find a suitable input x_b. This strategy produced well camouflaged attacks that were capable of fooling the detector at remarkable levels. The small changes also called perturbations are the major premise for adversarial images, these perturbations could be designed to create adversarial examples for each image in a dataset or a universal template that is capable of fooling an entire network of interest. We further placed these created adversarial images and placed them as patches on the images of interest as shown in Figure 2.

4.3 Experimentation

We built a DCNN detector capable of identifying target chips from non-target chips at a 99% accuracy level. The network was built using the VGG16 architecture as a template. We used the 40x74 target chips containing targets as well as chips containing clutter from the 480x720 image respectively. Both images were labelled accordingly to produce a detector prediction of target or not-target from the detector system. Armed with our detector system, we further crafted adversarial patches and appended them to each target of interest in the 480x720 image of the entire test dataset. The adversarial patches[?] were placed at specific points on the target

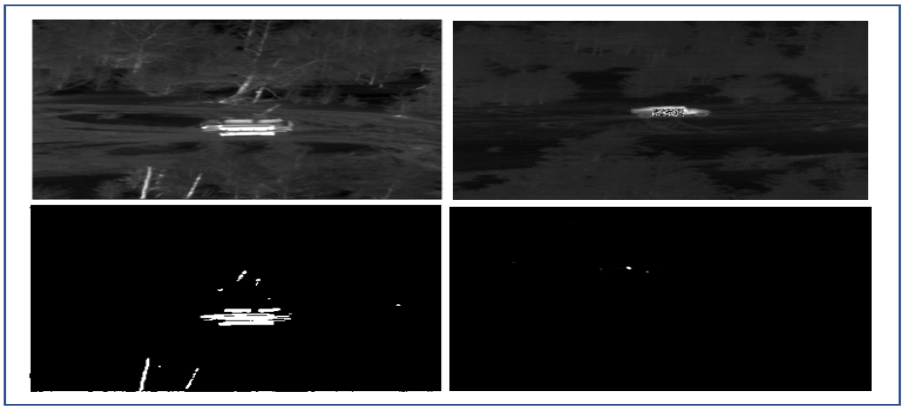

Figure 3: Generated heat map. The top-left image is fed into the network without any adversarial patch added to the target region and a corresponding heat-map is generated at the left-bottom image. However, in the top-right image, the target regions contain adversarial patches and a heat-map is generated (right bottom), indicating the inability of the detector to predict target spots due to the adversarial patch.

to maximize the attack approach (FGSM). This newly built images of the test data were then fed to the DCNN detector by striding through the 480x720 image in a 40x74 detector probe sliding fashion, where a prediction of 0 or 1 is assigned to background or target respectively on the each image frame. To evaluate the adversarial target detection system, we established a couple of strategies to test the integrity of the DCNN network. We used the Adam optimizer with $b1 = 0.5, b2 = 0.99$ and an initial learning rate of 0.0001. The learning rate was further decreased by about half for every 2,000 iterations. We ran our experiments on two NVIDIA TITAN X GPUs for 200 epochs with batch size of 16. Experiments were conducted for the entire combination dataset comprising of additional augmented images. The chip sizes (40x74) helped reduce issues related to computational complexity and memory management. A resulting heat map is generated at the output of the detector system indicating if the adversarial property is effective enough as to wrongly detect targets and assign the wrong labels as shown in Figure 3. We observed a similar trend of performance when we strictly compared the accuracy of the system over a range of perturbation (ϵ) values (Figure 4). We placed ϵ at two ranges ϵ_1(red) and ϵ_2(blue). The blue trend line confirms the adversarial property while the red line maintained a high accuracy level when the adversarial property is extremely negligible.

The response of the adversarial attack on the DCNN-detector is illustrated as an ROC-curve in Figure 5, the trade off between the intensity of perturbation ϵ and the visual appearance of the adversarial defines the level of accuracy for the network. We observed that the higher the intensity of the attack, the lower the accuracy performance of the system. We also attacked test image containing adversarial patches at different degrees of intensity ϵ, to test the sensitivity of the DCNN detection networks. As expected, the performance of the DCNN architecture dropped considerably by over 40%.

5. CONCLUSION

In this paper, we developed an algorithm for target detection for deep convolutional neural networks (DCNNs). we also crafted robust adversarial images to test the detection fidelity of the entire system. The detection system identifies potential targets in the FLIR image frame and produces a heat map that isolates the target of interest form clutter or image noise. The adversarial targets were generated by using each image as a variable in the loss function and gradient computations. The adversarial attack weakened the precision of detection at considerably high ratings. We also adapted all the necessary techniques to improve the detection potential of the network to over 98% before attacking. Our experimental results show that DCNNs are still susceptible to adversarial attacks, regardless of the quality of the detection system.

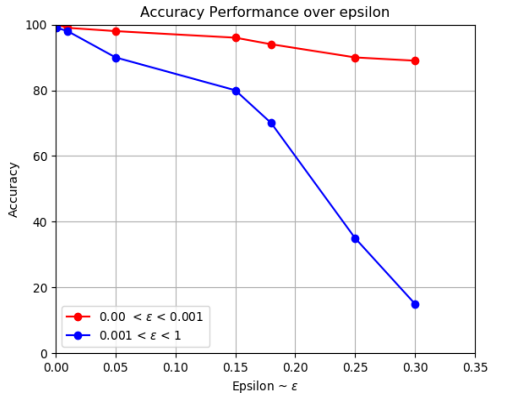

Figure 4: Accuracy plot. The accuracy of the system is shown for two ϵ ranges. the red line shows better accuracy levels at very small epsilon values ($0 < \epsilon < 0.001$) as compared to the blue line where ϵ ranges from ($0.001 < \epsilon < 1$). The downward trend of the blue plot confirms the impact of adversarial patches to the detector system.

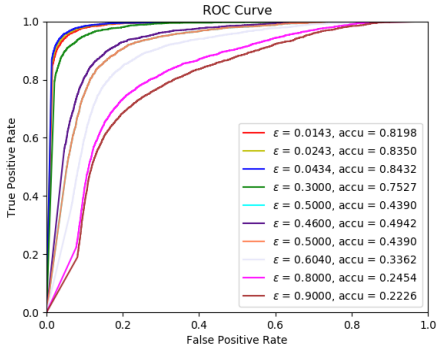

(a) Overall System

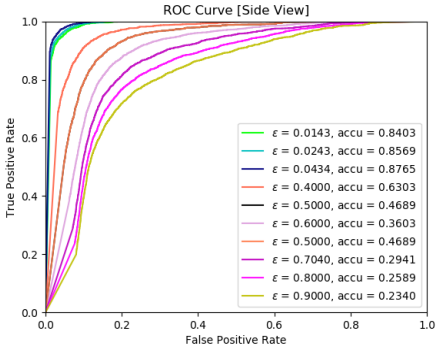

(b) Side view

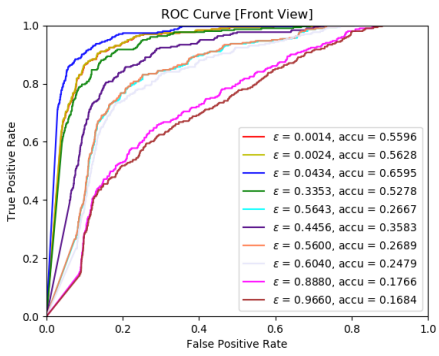

(c) Front view

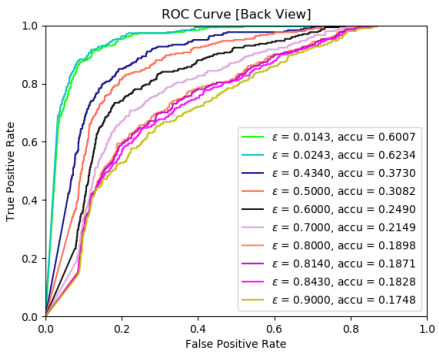

(d) Back view

Figure 5: ROC curve. The plots indicate the performance of the DCNN detector network over the four main orientations of the targets. (a) is an overall representation of the system performance over different values of adversarial perturbation intensity ϵ. (b,c,d) show the performance of the system for the side, frontal and back view over different adversarial intensities. The higher values of ϵ significantly reduced the prediction quality of the target detector.